Eurographics Conference on Visualization (EuroVis) (2015)
E. Bertini, J. Kennedy and E. Puppo (Editors)

Improved Sparse Seeding for 3D Electrostatic Field Lines

K. Scharnowski[1], S. Boblest[1], and T. Ertl[1]

[1]Visualization Research Center, University of Stuttgart, Germany

Abstract

We present an improved seeding strategy for sparse visualization of electrostatic fields. By analyzing the curvature of the field lines, we extract points of extremal field strength between charges of different sign and use them to seed field lines, which consequently connect the corresponding charges. The resulting sparse representation can be seen as an extension to classic vector field topology depicting properties otherwise hidden. Finally, by applying our method to a synthetic data set, we show its benefits over previously published work.

Categories and Subject Descriptors (according to ACM CCS): I.3.3 [Computer Graphics]: Picture/Image Generation—Line and curve generation J.2 [Physical Sciences and Engineering]: Physics—

1. Introduction

Static fields of point charges appear in physics in a broad range of applications connected both to Newton's theory of gravity and to electrostatics. In said situations, while the scalar potential plays an important role, it is often equally important to investigate force field properties, in particular by means of appropriate visualization techniques [SS96].

When visualizing 3D vector fields by means of a dense representation, visual clutter is inherent. A sparse representation, though, needs to be based on a meaningful and representative set of vector field features. A common way to achieve this are topological skeletons. However, existing methods for classic topological skeletons do not capture certain aspects of point-based force fields, namely, the interaction between two adjacent differently signed charges (DC). When following a field line between two adjacent DC, there will always be one point of minimal field magnitude, since the field magnitude diverges at the DC. The set of these minimal points forms a surface. A sparse representation of the interaction between the DC can thus be obtained by seeding a single field line at the location where the field strength is locally maximal with respect to this surface. This representation complies with the visual metaphor of drawing more dense field lines at locations of locally higher field strength that is often used in physical sciences and engineering for gravitational or electrostatic fields [WVHW96]. Mathematically equivalent to this, Handa *et al.* [HKT01] developed a seeding strategy based on points of extremal field magnitude and zero vector field curvature as an extension to classic vector field topology. However, we found examples of charge distributions where their technique fails to capture the full set of seed points. This happens in particular in cases where one of the DC takes part in a cluster consisting of several equally signed charges (EC) that are very close together, as might be the case in Molecular Dynamics simulations.

We present an improvement to the seeding strategy presented in [HKT01]. By generalizing their definition of critical points, we manage to create a more complete representation of the charge interaction. We apply our technique to a representative synthetic data set and highlight details that cannot be found by employing common visualizations for vector field topology or the method presented in [HKT01].

2. Related Work

Vector field topology was introduced by Helman and Hesselink [HH89] and later extended to the 3D case [GLL91]. Several authors have presented methods to create topological skeletons and other sparse representations of vector fields [LHZP07, PPF*11, TWHS03].

Previous work dealt with the visualization of both electrostatic fields and the more general electromagnetic fields. In [SCT*10, SCTC12] toroidal magnetic fields were investigated. In [Sun03], a dynamic line integral convolution for magnetic fields is presented, which exploits the equations of motion for test monopoles in electromagnetic fields to define the motion of field lines. This principle is also referred to in [BO03], where a mathematical discussion of field line velocity is given. Further related work deals with

DOI: 10.2312/eurovisshort.20151120

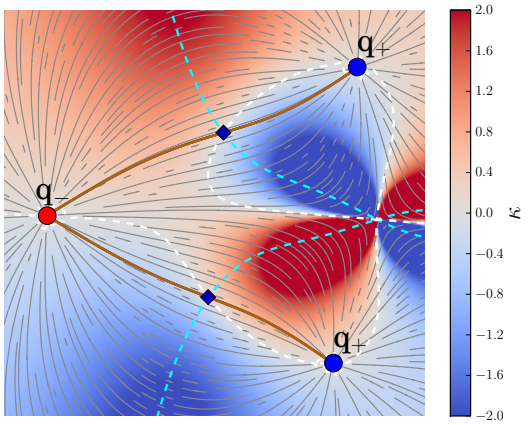

Figure 1: *A 2D electrostatic field based on three charges ($q_- = -1.0$ and $q_+ = 0.5$). The texture shows the curvature κ. In addition, the isoline for $\kappa = 0$ is shown in white (dashed) and the isoline for $\mathrm{d}|\mathbf{E}|/\mathrm{d}t = 0$ is shown in cyan (dashed). The intersection points of both isolines (diamond) are used as seed points.*

solar dynamics data [MSM*12] or dipole fields [GBM*12]. In [THK*05], a technique is presented to extract higher order critical points from vector fields, more specifically, the electrostatic field of a benzene-molecule. Furthermore, it has been shown that critical points can be extracted analytically from point based vector fields if the locations of the point charges are known [MW09].

Close in spirit to our work is the technique presented in [BSW*12], where 2D magnetic flux topology is introduced. The algorithm is based on finding Morse-Smale cells in a dual field and choosing a representative seed point based on the mean potential. Similarly, we could search for Morse-Smale cells in our data, since every field line that connects two DC is inside a Morse-Smale cell of the electrostatic force force field. An alternative would be to analyze the basins of attraction for the individual point charges. However, both of these approaches are computationally heavy and do not agree with our aim to only use local computations for seed point generation. Furthermore, we would still need to find a distinctive criterion to choose a field line for each connected pair of DC to make visualizations of different data sets coherent and, thus, comparable. Our method is an extension to the algorithm presented by Handa *et al.* [HKT01], who have presented a seeding strategy for electrostatic fields that extracts a sparse set of seed points using local vector field properties.

3. Theoretical Background

Force fields created by systems of point charges appear in various applications in physics. Interaction between electrically charged or massive bodies can be described by an electrostatic or gravitational potential ϕ. In both cases, the corresponding force field is defined as the negative gradient of the potential function, $\mathbf{E} = -\nabla\phi$, and has the form

$$\mathbf{E}(\mathbf{r}) = C \sum_{i=1}^{N} Q_i \frac{\mathbf{r} - \mathbf{r}_i}{|\mathbf{r} - \mathbf{r}_i|^3} \tag{1}$$

for N particles. Here, Q_i are the masses or electric charges at the locations $\mathbf{r}_i$, respectively, and C is a constant that depends both on the type of field and the units used. The point charges are sources or sinks of the field depending on their sign. The real field $\mathbf{E}$ diverges at the locations of the point charges, however, as we use linear interpolation, this behavior is not reflected in our data.

4. Field Line Seeding

In [HKT01], Handa *et al.* introduce a new class of critical points that can be seen as an extension to the classic topological skeleton by Helman and Hesselink [HH89]. This new class of points is based on the observation that each field line that connects DC contains a point where the field magnitude $|\mathbf{E}|$ becomes minimal while $\mathbf{E}$ does not vanish (see Figure 1). These points cannot be found using conventional methods, which require $\mathbf{E} = \mathbf{0}$.

The set of all points with extremal field magnitude forms an isosurface

$$\mathcal{I} = \left\{ \mathbf{p} \in \mathbb{R}^3 \,\middle|\, \frac{\mathrm{d}|\mathbf{E}(\mathbf{p}(t))|}{\mathrm{d}t} = 0 \right\}, \tag{2}$$

where t represents a parametrization of the respective tangent curve. $\mathcal{I}$ is pierced by all field lines connecting a pair of DC (c.f. Figure 1). A sparse representation of DC interaction can then be created by choosing a suitable subset of this set of lines. To this end, Handa *et al.* propose an alternative formulation of the problem of finding critical points using the directional derivative of $\mathbf{E}$ (refer to [HKT01] for a detailed derivation). According to the new formulation, critical points in $\mathbf{E}$ are given by

$$\frac{\mathrm{d}\mathbf{E}}{\mathrm{d}t} = \frac{\mathrm{d}|\mathbf{E}|}{\mathrm{d}t}\mathbf{e}_1 + |\mathbf{E}|^2\kappa\mathbf{e}_2 = \mathbf{0}. \tag{3}$$

This includes regular critical points where $|\mathbf{E}| = 0$. From Eq. (3) follows that critical points with $|\mathbf{E}| > 0$ are characterized by $\mathrm{d}|\mathbf{E}|/\mathrm{d}t = 0$ and $\kappa = 0$ (c.f. Figure 1). Hence, the algorithm chooses from all points on $\mathcal{I}$ those with zero curvature. Handa *et al.* refer to these new critical points as *dynamic critical points* and we adopt this term in the remainder of this paper. Note that, while κ is undefined at locations of regular critical points, it is well-defined at locations of dynamic critical points, since there $|\mathbf{E}(t)| > 0$.

We noticed that, while the method of Handa *et al.* allows to capture connective field lines for DC in most cases, it fails to extract them between clusters of charges (where some EC are sufficiently close to each other), since not all of the interactions lead to a zero curvature point on $\mathcal{I}$. We, therefore,

propose to extend the set of points given by Eq. (3) to contain locations on $\mathcal{I}$, where κ is locally minimal on $\mathcal{I}$.

In order to find our newly defined seed points, we compute κ and its partial derivatives in Euclidean space projected to $\mathcal{I}$. We explicitly compute the curvature κ of the field lines using $\mathbf{E}$ and its directional derivative $\mathrm{d}\mathbf{E}/\mathrm{d}t$ as proposed in [Far02, WT02] by

$$\kappa(t) = \frac{|\mathbf{E}(t) \times \mathrm{d}\mathbf{E}/\mathrm{d}t|}{|\mathbf{E}(t)|^3}. \tag{4}$$

The projected gradient $\mathbf{w}$ is defined by

$$\mathbf{w} = \nabla\mathcal{I} \times (\nabla\kappa \times \nabla\mathcal{I}). \tag{5}$$

In order to extract a set of potential seed points, we first search for null points of the vector fields

$$v_1 = \begin{pmatrix} \mathrm{d}|\mathbf{E}|/\mathrm{d}t \\ w_x \\ w_y \end{pmatrix}, v_2 = \begin{pmatrix} \mathrm{d}|\mathbf{E}|/\mathrm{d}t \\ w_y \\ w_z \end{pmatrix}, v_3 = \begin{pmatrix} \mathrm{d}|\mathbf{E}|/\mathrm{d}t \\ w_x \\ w_z \end{pmatrix} \tag{6}$$

using Newton-Raphson iteration. Subsequently, we classify the found points by computing a 2D-Jacobian with respect to a local tangential parametrization of $\mathcal{I}$ and take all points that are local minima of κ on $\mathcal{I}$, which includes the points found by Handa *et al.* Furthermore, we omit points that emerge twice at the same position, which happens, e.g., when $\nabla\kappa = \mathbf{0}$, hence at the original dynamic critical points. Finally, we follow Handa *et al.* in classifying the dynamic critical points as *minimum* (for $\mathrm{d}^2|\mathbf{E}|/\mathrm{d}t^2 > 0$) and *maximum* (for $\mathrm{d}^2|\mathbf{E}|/\mathrm{d}t^2 < 0$) extreme points, respectively. For us, minima are particularly important, since they act as a representation of interaction between two DC.

While our approach concentrates on the interaction between DC, we do not want to neglect the relation of adjacent EC. This relation is particularly relevant in vector fields that contain only sinks or only sources (e.g. in gravitational fields). We, therefore, combine our connective field lines with separation surfaces and streamlines in the outflow and inflow directions to represent saddles in the field $\mathbf{E}$. This rather simple visualization representing classic vector field topology is sufficient for our input data. In more complicated vector fields further simplification of the topology (e.g. [THK*05]) or more sophisticated visualizations (e.g. [TWHS03]) might be necessary.

5. Results

We now compare the results of our method with ones obtained by using the method of Handa *et al.* We use a synthetic data set containing a neutral system of three particles with $p_1 = (-1.5,\ -0.75,\ 0.05)$, $p_2 = (1.5,\ -\gamma,\ 0.05)$, and $p_3 = (1.5,\ +\gamma,\ 0.05)$, as well as $q_1 = -1.0$ and $q_{2,3} = 0.5$, where $0.0 \leq \gamma \leq 1.5$. $\mathbf{E}$ is computed using Eq. (1), with $C = 1$ and is sampled on a grid $(200 \times 182 \times 108)$. The bounding box is originated at $(-1.75, -1.7, -1.0)$ with side lengths $l_x = 3.75$, $l_y = 3.4$, and $l_z = 2.0$. A continuous representation is obtained by linear interpolation. Furthermore, we use a fourth order Runge-Kutta scheme for all integration steps.

When gradually decreasing γ, we can make out three phases. Figure 2 shows key moments of this development. Phase one lasts from $\gamma \geq 1.5$ to $\gamma \gtrsim 1.005$ (Figures 2a, 2b). Here, both methods deliver the desired result of two distinct connective field lines (based on the minimal dynamic critical points) for both pairs of DC. Phase two lasts from $\gamma \approx 1.005$ to $\gamma \approx 0.825$ (Figures 2b, 2c, 2d). During this phase the curvature zero line penetrates $\mathcal{I}$ only in one location of minimal field strength. Consequently, the method of Handa *et al.* leads to one connective field line based on this location. There is also a maximum dynamic critical point that is found near the saddle point between the two EC. Our method finds an additional minimum point (in cyan, see arrow). Figure 2b captures the moment where this additional minimal point emerges from the maximum point. Phase three lasts from $\gamma \lesssim 0.825$, where the additional minimum found by our method vanishes, to $\gamma = 0$ (Figures 2e, 2f). Subsequently, neither our method, nor the one by Handa *et al.* lead to two minimal dynamic extremal points. Finally, for $\gamma = 0$ we obtain one line connecting the negative charges and the (now superimposed) positive charges as expected.

6. Conclusion & Future Work

We presented an improved seeding strategy that creates a sparse representation of the interaction between adjacent DC in electrostatic fields, thereby complementing conventional vector field topology. By applying the method to a representative synthetic data set, we showed that our method delivers better results in comparison with previous work, which failed to deal with closely-packed clusters of EC. Nonetheless, we still found cases, where both previous work and our approach fail to find all the desired features. Therefore, creating a complete representation of all the interactions between DC (including close-packed clusters) remains a challenge and is subject to future work.

In addition, we want to investigate possibilities to extend the approach to more general (non-irrotational) fields. Particularly, we want to consider the electrodynamic case, where electric and magnetic fields necessarily have to be treated together. Furthermore, we plan to apply our method to more complicated force fields, for example in the context of Molecular Dynamics simulations, testing the robustness of the seeding strategy more extensively with different numerical approaches (e.g. PME, Coulomb summation).

Acknowledgments

This work is partially funded by DFG as part of SimTech and BMBF as part of HONK.

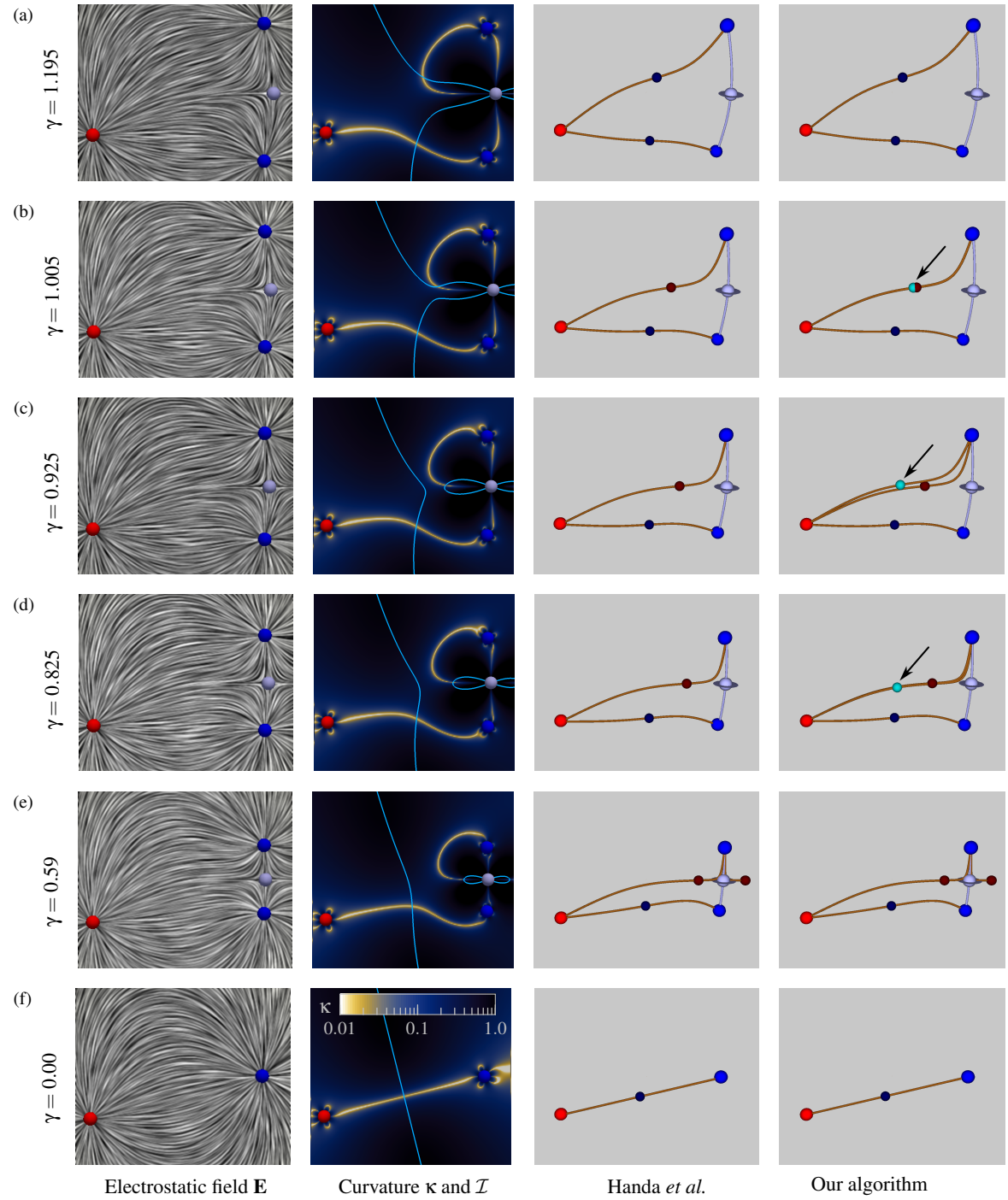

Figure 2: *A synthetic 3D data set consisting of three point charges. Column one shows the electrostatic field* **E**. *Column two shows a texture slice of the curvature* κ *in combination with an isoline representing* $\mathcal{I}$. *Columns three and four (camera tilted slightly) show the seeding technique of Handa et al. [HKT01] and our improved method in comparison. Dynamic critical points found by both methods are dark blue (for minimal points) and dark red (for maximal points), respectively. Points found only by our algorithm are shown in cyan (arrow). The pictures in columns one and two were created using ParaView [HA04].*

References

[BO03] BELCHER J. W., OLBERT S.: Field line motion in classical electromagnetism. *American Journal of Physics 71*, 3 (Mar. 2003), 220–228. doi:10.1119/1.1531577. 1

[BSW*12] BACHTHALER S., SADLO F., WEEBER R., KANTOROVICH S., HOLM C., WEISKOPF D.: Magnetic Flux Topology of 2D Point Dipoles. *Computer Graphics Forum 31*, 3pt1 (June 2012), 955–964. doi:10.1111/j.1467-8659.2012.03088.x. 2

[Far02] FARIN G.: *Curves and Surfaces for CAGD: A Practical Guide*, 5th ed. Morgan Kaufmann Publishers Inc., San Francisco, CA, USA, 2002. 3

[GBM*12] GROTTEL S., BECK P., MÜLLER C., REINA G., ROTH J., TREBIN H.-R., ERTL T.: Visualization of Electrostatic Dipoles in Molecular Dynamics of Metal Oxides. *IEEE Transactions on Visualization and Computer Graphics 18*, 12 (2012), 2061–2068. doi:10.1109/TVCG.2012.282. 2

[GLL91] GLOBUS A., LEVIT C., LASINSKI T.: A Tool for Visualizing the Topology of Three-dimensional Vector Fields. In *Proceedings of the 2nd Conference on Visualization '91* (Los Alamitos, CA, USA, 1991), VIS '91, IEEE Computer Society Press, pp. 33–40. 1

[HA04] HENDERSON A., AHRENS J.: *The Paraview Guide : A Parallel Visualization Application*. Kitware, Inc., New York, 2004. URL: http://opac.inria.fr/record=b1117983. 4

[HH89] HELMAN J. L., HESSELINK L.: Representation and Display of Vector Field Topology in Fluid Flow Data Sets. *Computer 22*, 8 (Aug. 1989), 27–36. doi:10.1109/2.35197. 1, 2

[HKT01] HANDA S., KASHIWAGI H., TAKADA T.: Visualization techniques for 3D vector fields: an application to electrostatic fields of molecules. *The Journal of Visualization and Computer Animation 12*, 3 (2001), 167–180. doi:10.1002/vis.255. 1, 2, 4

[LHZP07] LARAMEE R. S., HAUSER H., ZHAO L., POST F. H.: Topology-Based Flow Visualization, The State of the Art. In *Topology-based Methods in Visualization*, Hauser H., Hagen H., Theisel H., (Eds.), Mathematics and Visualization. Springer Berlin Heidelberg, 2007, pp. 1–19. doi:10.1111/j.1467-8659.2011.01901.x. 1

[MSM*12] MACHADO G. M., SADLO F., MÜLLER T., MÜLLER D., ERTL T.: Visualizing Solar Dynamics Data. In *VMV'12* (2012), pp. 95–102. doi:10.2312/PE/VMV/VMV12/095-102. 2

[MW09] MAX N., WEINKAUF T.: Critical Points of the Electric Field from a Collection of Point Charges. In *Topology-Based Methods in Visualization II*, Hege H.-C., Polthier K., Scheuermann G., (Eds.), Mathematics and Visualization. Springer, 2009, pp. 101–114. doi:10.1007/978-3-540-88606-8_8. 2

[PPF*11] POBITZER A., PEIKERT R., FUCHS R., SCHINDLER B., KUHN A., THEISEL H., MATKOVIĆ K., HAUSER H.: The State of the Art in Topology-Based Visualization of Unsteady Flow. *Computer Graphics Forum 30*, 6 (2011), 1789–1811. doi:10.1111/j.1467-8659.2011.01901.x. 1

[SCT*10] SANDERSON A. R., CHEN G., TRICOCHE X., PUGMIRE D., KRUGER S., BRESLAU J.: Analysis of Recurrent Patterns in Toroidal Magnetic Fields. *IEEE Transactions on Visualization and Computer Graphics 16*, 6 (Dec. 2010), 1431–1440. doi:10.1109/TVCG.2010.133. 1

[SCTC12] SANDERSON A., CHEN G., TRICOCHE X., COHEN E.: Understanding Quasi-Periodic Fieldlines and Their Topology in Toroidal Magnetic Fields. In *Topological Methods in Data Analysis and Visualization II*, Peikert R., Hauser H., Carr H., Fuchs R., (Eds.), Mathematics and Visualization. Springer Berlin Heidelberg, Jan. 2012, pp. 125–140. doi:10.1007/978-3-642-23175-9_9. 1

[SS96] STALLING D., STEINKE T.: *Visualization of Vector Fields in Quantum Chemistry*. Tech. rep., Zuse Institut, Berlin, 1996. 1

[Sun03] SUNDQUIST A.: Dynamic line integral convolution for visualizing streamline evolution. *IEEE Transactions on Visualization and Computer Graphics 9*, 3 (July 2003), 273–282. doi:10.1109/TVCG.2003.1207436. 1

[THK*05] T. WEINKAUF, H. THEISEL, K. SHI, H.-C. HEGE, H.-P. SEIDEL: Extracting Higher Order Critical Points and Topological Simplification of 3D Vector Fields. In *Proceedings of IEEE Visualization'05* (Minneapolis, U.S.A., Oct. 2005), pp. 559–566. doi:10.1109/VISUAL.2005.1532842. 2, 3

[TWHS03] THEISEL H., WEINKAUF T., HEGE H.-C., SEIDEL H.-P.: Saddle Connectors - An Approach to Visualizing the Topological Skeleton of Complex 3D Vector Fields. In *Proceedings of IEEE Visualization'03* (Seattle, U.S.A., October 2003), pp. 225–232. doi:10.1109/VISUAL.2003.1250376. 1, 3

[WT02] WEINKAUF T., THEISEL H.: Curvature Measures of 3D Vector Fields and Their Applications. *Journal of WSCG 10* (2002), 507–514. 3

[WVHW96] WOLF A., VAN HOOK S. J., WEEKS E. R.: Electric field line diagrams don't work. *American Journal of Physics 64*, 6 (1996), 714–724. doi:10.1119/1.18237. 1